Amyloid Fibrils

Measurement of Amyloid Fibril Length Distributions by Inclusion of Rotational Motion in Solution NMR Diffusion Measurements**

Andrew J. Baldwin, Spencer J. Anthony-Cahill, Tuomas P. J. Knowles, Guy Lippens, John Christodoulou, Paul D. Barker, and Christopher M. Dobson

Supramolecular assemblies and other nanoscale structures fall within a range of characteristic length scales, where, in contrast to the situation for smaller molecular species, rotational motion provides an important contribution to particle displacement in addition to translational diffusion.[1] Herein we demonstrate that this effect not only has profound implications for the interpretation of NMR diffusion experiments, but can also be used to provide the basis for a new approach for measuring length distributions of high-aspect ratio molecular assemblies, such as amyloid fibrils, in situ. The ability to make such measurements is of very considerable importance as accurate length determination of biological filaments in solution remains an extremely challenging task, and the commonly used microscopy-based approaches require transfer of the structures from solution to a surface prior to analysis. We have studied fibrils of an SH3 domain fused to apo-cytochrome b$_{562}$ (apo-(SH3)$_2$Cyt),[2] and demonstrate that the lengths obtained using our NMR method are comparable to, but slightly larger than, those measured using atomic force microscopy (AFM) and transmission electron microscopy (TEM) following deposition on a surface. We discuss the implications of this finding for the definition of the sizes of nanoscale biological components in solution.

The flexible regions of a number of large biomolecular systems, including multidomain enzymes,[3,4] molecular chaperones,[5] intact ribosomes,[6,7] and noncore residues of amyloid fibrils[2,8,9] have been characterized by solution-state NMR spectroscopy. Although the size of such species can greatly exceed the usual limits for solution-state NMR methods, the "motional narrowing" resulting from local mobility can be sufficient to average almost completely the internal dipolar interactions that normally dominate the transverse relaxation rates.[2–8] Resonances from such states may then have linewidths comparable to those of free peptides in solution, making possible the application of a wide range of NMR techniques.

One type of experiment of particular value for the study of large complexes involves the use of pulsed field gradients (PFGs) to measure translational diffusion coefficients and thus estimate their molecular dimensions.[10] In studies of amyloid fibrils, however, we observed anomalies in such measurements. We prepared and purified fibrils of apo-(SH3)$_2$Cyt[2] as described in the Supporting Information, Section S1. TEM analysis revealed structures typical of amyloid assemblies with widths of ca. 10 nm, and a range of lengths in the vicinity of 2 μm (Figure 1a). These fibrillar species[2] were found to yield well-resolved solution-state NMR spectra, a situation that can be attributed to the fast dynamics of the substantially unfolded cytochrome component in the fibrils (Figure 1b). Pulsed-field gradient stimulated echo (PFGSE) NMR data were then recorded with a conventional diffusion delay ($\Delta = 100$ ms) and analysed using the Stejskal–Tanner (ST) equation,[11]

$$D_{eff} \% G^2 = -\frac{1}{\alpha^2 \beta} \ln \frac{S_i}{S_0} \tag{1}$$

where $D_{eff} = D_T$. This equation relates the signal intensity in the presence S_i and absence S_0 of the applied gradients of field strength G, measured as a fraction of the maximum gradient G_{max} that is applied, such that $\% G = G/G_{max}$, to the translational diffusion coefficient D_T of the sample under study, where $\alpha = \gamma \delta G_{max}$, $\beta = \Delta - \delta/3$, γ is the gyromagnetic ratio of the nucleus under study, δ is the gradient duration, and Δ is the diffusion delay. The values of D_T calculated in this manner were found to be sample dependent (Figure 1c) and the values of R_H (Figure 1d, 2–12 nm) determined from D_T using the Einstein-Stokes equation (Supporting Information, S2), were approximately three orders of magnitude less than the fibril lengths observed by TEM.

When NMR spectra were acquired with an exceptionally long diffusion delay ($\Delta = 1$ s), the resonances of monomeric apo-(SH3)$_2$Cyt were clearly visible at 10% G_{max} but were effectively completely suppressed by 50% G_{max} (Figure 1b, top). Remarkably, only modest attenuation of the signal intensity was observed between the spectra of fibrillar apo-(SH3)$_2$Cyt at 10% and 50% G_{max} (Figure 1b, bottom). Fitting

[*] A. J. Baldwin, S. J. Anthony-Cahill, J. Christodoulou, P. D. Barker, C. M. Dobson
Department of Chemistry
University of Cambridge
Lensfield Road, Cambridge, CB2 1EW (UK)
Fax: (+ 44) 1223 336-362
E-mail: cmd44@cam.ac.uk

T. P. J. Knowles
Centre for Nanoscience and Cavendish Laboratory
University of Cambridge
Madingley Road, Cambridge, CB3 0FF (UK)

G. Lippens
UMR8576, CNRS
59655, Villeneuve d'Ascq (France)
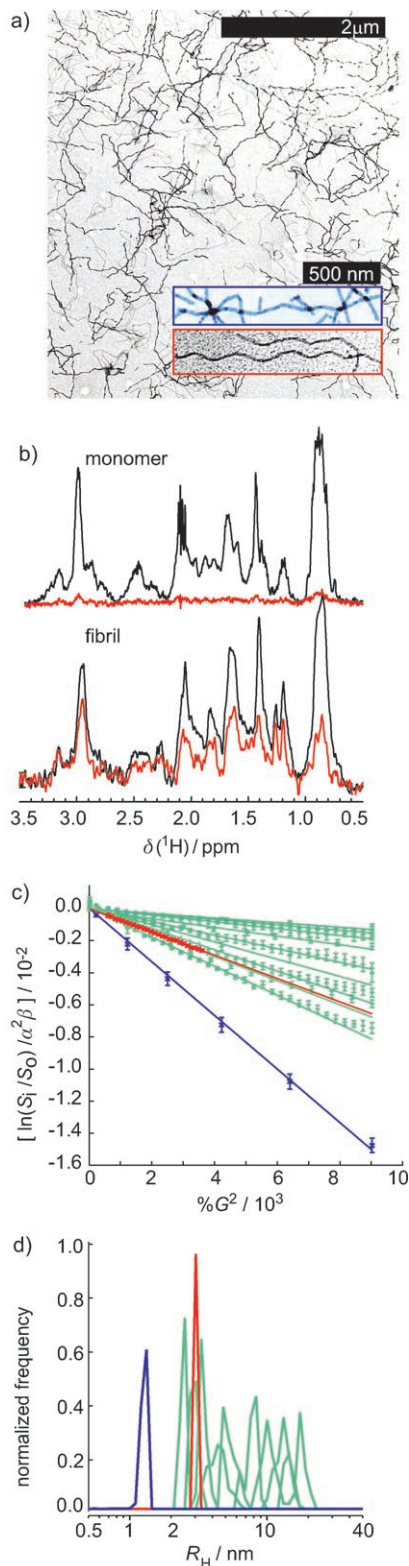
Figure 1. a) Appearance of apo-(SH3)$_2$Cyt fibrils. Insets: TEM (red) and AFM (blue) images of individual fibrils. b) ^{1}H PFGSE NMR spectra of monomeric (top) and fibrillar (bottom) apo-(SH3)$_2$Cyt. In both cases $\Delta = 1$ s and $\delta = 5.4$ ms with 10% (black) and 50% (red) of the maximum gradient. c) Integrated PFGSE profiles recorded with $\Delta = 100$ ms using samples of apo-(SH3)$_2$Cyt fibrils at various incubation times (green), monomeric apo-(SH3)$_2$Cyt (red), and human lysozyme (blue). Data are fitted to the ST equation. d) An alternative representation of the same data, converting D_T into R_H, with the width of the trace indicating the experimental uncertainty (Supporting Information, S2).

these data as above yields an R_H value of 165 nm, a result inconsistent both with the fibril lengths observed by TEM and the R_H estimate obtained with $\Delta = 100$ ms.

PFGSE NMR experiments measure directly the net physical displacement of nuclear spins.[10] For large systems where at least one length dimension exceeds 500 nm, the displacement resulting from rotational diffusion is similar to, and indeed can exceed, the contribution from translational diffusion (Supporting Information, S3). Thus, the influence of rotational motion must be considered explicitly when analyzing NMR diffusion data for large systems. To interpret the data for the amyloid fibrils studied in this work, the fibrils were considered to be rigid rods, and whose initial and final orientations were independent of each other.[1] In this limiting case, displacements arising from rotational motion will be independent of the diffusion delay time, but those due to translational motion will increase. Under these conditions, an expression for an effective diffusion coefficient can be derived:[1]

$$D_{\text{eff}} = D_T + \frac{1}{\alpha^2 \beta} \ln \frac{\sin^2(\alpha L)}{(\alpha L)^2} \tag{1}$$

where L is the distance of a given spin from the centre of mass. The second term in Equation (2) predicts an additional attenuation in signal intensity arising from rotational diffusion, leading to larger effective diffusion coefficients at shorter diffusion delays. In the limit $\alpha L \rightarrow 0$, rotational effects are negligible, and Equation (2) reduces to the ST equation where $D_{\text{eff}} = D_T$.

The effects of varying the diffusion delay on the intensities of resonances in the NMR spectra of apo-(SH3)$_2$Cyt in its fibrillar and monomeric states are shown in Figure 2a. When plotted as shown, ST behavior predicts that all integrated signal intensities should lie on a single line for all diffusion delays. Such a situation is found for monomeric apo-(SH3)$_2$Cyt (red), where a diffusion coefficient corresponding to $R_H = (2.8 \pm 0.6)$ nm is obtained (Figure 2b and c, red), but not for fibrillar apo-(SH3)$_2$Cyt (green).

To analyze the fibril data, a function with two exponential terms was fitted to the intensity profiles (Figure 2a, green), yielding two effective diffusion coefficients. The larger of these coefficients is similar to that of monomeric apo-(SH3)$_2$Cyt, and can be attributed to a small population of monomeric material that exchanges with the fibrils but on a timescale of weeks. The smaller of the effective diffusion coefficients for fibrillar apo-(SH3)$_2$Cyt (Figure 2b, green) becomes less than that of monomeric apo-(SH3)$_2$Cyt only when $\Delta \geq 100$ ms. Assuming that the NMR signal originates from molecules distributed evenly over the length of the fibril, summing Equation (2) over the length of a rod gives an expression from which the fibril lengths can be estimated (Supporting Information, S4), and which is largely independent of the theoretical model used for D_T (Supporting Information, S4). The best fit, using this model (Figure 2b, green line) corresponds to a length of 12 μm (Figure 2c, black), a value comparable to the longest fibrils seen in AFM and TEM experiments.
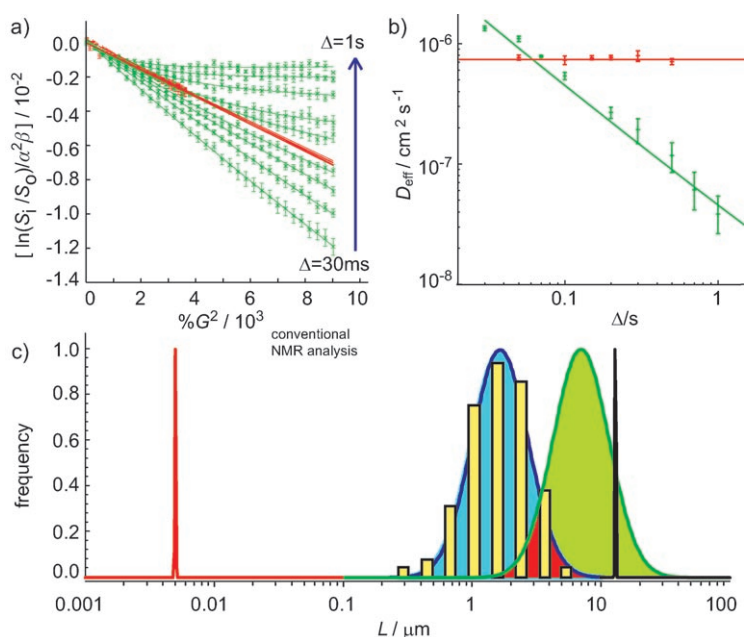
Figure 2. a) Integrated PFGSE profiles as a function of field strength for a range of values of Δ. Data from monomeric apo-(SH3)$_2$Cyt (red) fit well to the ST model, but those from fibril samples show marked deviations from it (green). b) The decay constants of the monomer (red) are independent of diffusion delay. The smaller decay constant (green) for the fibrils is strongly dependent on this delay. The fit (green line) is to Equation (1) as described in the text. c) Histogram (yellow) showing the length distribution obtained from statistical analyses of AFM and TEM images. Fits using the method described here to a single-rod model (black) and log–normal length distribution model (green) are shown. Fitting the NMR data using a conventional analysis (red) dramatically underestimates the fibril length L.

Analysis of AFM and TEM images shows that fibrils studied in this work are not of uniform length, and that the length distributions measured using these two techniques are statistically identical. To take such heterogeneous fibril lengths into account in the interpretation of the NMR data, Equation (2) was further refined to include a log–normal function specified by two independent variables a_0 and a_1, which together describe the centre and width of the distribution (Supporting Information, S4). The resulting distribution ($a_0 = 9$ μm, $a_1 = 0.6$) obtained from fitting this model to the NMR data (Figure 2c, green) has χ^2 values significantly lower than that for the single-rod model. Although the width of the length distribution measured by the NMR method closely matches that from AFM and TEM, and the two distributions overlap, the most probable length (9 μm) is still significantly greater than that observed by AFM and TEM (2 μm). Previous observations have shown that fibrils of the type studied here are readily fractured.[12–14] The differences between the solution-state measurements and the microscopic data are therefore likely to be due, at least in part, to breakage of fibrils during the surface deposition process.[12]

In conclusion, the inclusion of the effects of rotational diffusion in the analysis of NMR diffusion data (Figure 2c) yields an estimate of the lengths of fibrils that is of the same order of magnitude as that measured by AFM and TEM.

Using the conventional analysis of NMR diffusion data (Figure 1d), fibril lengths of the system studied herein are underestimated by three orders of magnitude. These results provide a clear example of the effects of rotational diffusion on NMR PFGSE measurements and reveal the potential value of this phenomenon for characterizing such species in solution. This approach is readily applicable to the study of any large molecular structure by solution-state NMR spectroscopy provided that at least one dimension exceeds ca. 500 nm, and that the local molecular dynamics permit resonances to be observed. The technique provides a powerful method for probing noninvasively the distribution of sizes of large molecular assemblies in solution, and indeed for observing changes in size as a function of time and solution conditions. In the present case it has enabled the distribution of lengths of a preparation of amyloid fibrils to be defined in the solution state, information that is essential for understanding in detail the kinetics and mechanism of fibril growth.[14]

[1] A. J. Baldwin, J. Christodoulou, P. D. Barker, C. M. Dobson, G. Lippens, *J. Chem. Phys.* **2007**, *127*, 114505.

[2] A. J. Baldwin, R. Bader, J. Christodoulou, C. E. MacPhee, C. M. Dobson, P. D. Barker, *J. Am. Chem. Soc.* **2006**, *128*, 2162.

[3] S. E. Radford, E. D. Laue, R. N. Perham, J. S. Miles, J. R. Guest, *Biochem. J.* **1987**, *247*, 641.

[4] R. E. Oswald, M. J. Bogusky, M. Bamberger, R. A. Smith, C. M. Dobson, *Nature* **1989**, *337*, 579.

[5] J. A. Carver, J. A. Aquilina, R. J. Truscott, G. B. Ralston, *FEBS Lett.* **1992**, *311*, 143.

[6] J. Christodoulou, G. Larsson, P. Fucini, S. R. Connell, T. A. Pertinhez, C. L. Hanson, C. Redfield, K. H. Nierhaus, C. V. Robinson, J. Schleucher, C. M. Dobson, *Proc. Natl. Acad. Sci. USA* **2004**, *101*, 10949.

[7] F. A. Mulder, L. Bouakaz, A. Lundell, M. Venkataramana, A. Liljas, M. Akke, S. Sanyal, *Biochemistry* **2004**, *43*, 5930.

[8] A. Sillen, A. Leroy, J. M. Wieruszeski, A. Loyens, J. C. Beauvillain, L. Buee, I. Landrieu, G. Lippens, *ChemBioChem* **2005**, *6*, 1849.

[9] S. Meehan, T. P. J. Knowles, A. J. Baldwin, J. F. Smith, A. M. Squires, P. Clements, T. M. Treweek, H. Ecroyd, G. G. Tartaglia, M. Vendruscolo, C. E. MacPhee, C. M. Dobson, J. A. Carver, *J. Mol. Biol.* **2007**, *372*, 470.

[10] A. Dehner, H. Kessler, *ChemBioChem* **2005**, *6*, 1550.

[11] E. O. Stejskal, J. E. Tanner, *J. Chem. Phys.* **1965**, *42*, 288.

[12] F. R. Hallett, R. Keates, *Biopolymers* **1985**, *24*, 2403.

[13] N. Carulla, G. L. Caddy, D. R. Hall, J. Zurdo, M. Gairi, M. Feliz, E. Giralt, C. V. Robinson, C. M. Dobson, *Nature* **2005**, *436*, 554.

[14] J. F. Smith, T. P. J. Knowles, C. M. Dobson, C. E. MacPhee, M. E. Welland, *Proc. Natl. Acad. Sci. USA* **2006**, *103*, 15806.